Production of Polystyrene Microcellular Foam Plastics and a Comparison of Late- and Quick-Heating

SUMARNO, YOSHIYUKI SATO, SHIGEKI TAKISHIMA, HIROKATSU MASUOKA

Chemical Engineering Thermodynamics Laboratory, Department of Chemical Engineering, Hiroshima University, 1-4-1 Kagamiyama, Higashi-Hiroshima 739-8527, Japan

Received 11 May 1999; accepted 16 September 1999

ABSTRACT: A batchwise process for the production of microcellular plastics was studied in the polystyrene–nitrogen system. The effects of saturation temperature, saturation pressure, and late- and quick-heating on the microcellular structure were investigated by considering the solubility of the gas in the polymer. It was found that the mean cell diameter was reduced and the cell number density increased with increase in the gas solubility. Variation in the saturation temperature showed that the cell number density had a minimum and the mean cell diameter had a maximum at about 350 K, which was related to the minimum solubility of nitrogen in polystyrene. The long heating time at 393 K of a solution saturated under 25 MPa increased the cell diameter, reduced the cell number density, and gave a maximum volume expansion ratio at about 300 s. Further heating caused the cell size and volume expansion ratio to be decreased, which might be caused by diffusion of the gas out of the polymer sample. The effect of the saturation temperature under high saturation pressure on the cell number density was qualitatively well predicted by the nucleation theory. © 2000 John Wiley & Sons, Inc. J Appl Polym Sci 77: 2383–2395, 2000

Key words: polystyrene; microcellular; late-heating; quick-heating, nucleation

INTRODUCTION

Microcellular plastic is a newly invented polymeric foam material that has several superior mechanical and thermal properties over conventional foam plastics. The characteristics of this material are the cell size over the range of 0.1 to 10 μm and the cell number density of 10^9 to 10^{15} cell/cm^3.[1] The cells are formed by bringing a saturated polymer–gas solution into a thermodynamically unstable state, where the solubility of the gas is instantaneously reduced by a decompression and/or a heating process. The use of environmentally benign gases such as carbon dioxide (CO_2) or nitrogen (N_2) instead of chlorofluorocarbons (CFC) or volatile organic compounds is a proper choice and urgently needed in the industrial production of foam plastics because of the necessity to develop an environmentally clean and safe production process.

Martini et al.[2] studied the effect of process conditions, such as initial gas concentration, heating temperature, and heating time on a polystyrene–nitrogen (PS–N_2) system. Cell sizes ranging from 0.1 to 25 μm and void fractions up to 30% were obtained by varying the process conditions. The cell size increased with increase in the heating temperature and heating time. A theoretical study on the nucleation of cells in a microcellular plastic based on the classical nucleation the-

Correspondence to: H. Masuoka (<masuoka@hiroshima-u.ac.jp.>).

A portion of this work was presented at the 5th Meeting on Supercritical Fluids, Nice, France, 1998.

Contract grant sponsor: Hiroshima Industrial Technology Organization and Japan Science and Technology Corp.

Journal of Applied Polymer Science, Vol. 77, 2383–2395 (2000)

ory was also undertaken. Colton and Suh[3] extended the classical nucleation theory by considering the free-volume effects due to additives and gases in a solution of the PS–N_2 system. They found that there were three regions of nucleation: a homogeneous region below the solubility limit of the additive of zinc stearate in PS (approximately 0.3%), a heterogeneous region above the solubility limit, and a mixed-mode region around the solubility limit. Theoretical treatment shows an overprediction at high pressure, but underprediction at low pressure.

Kumar and Suh[4] reported on experimental results of the nucleation of cells in the PS–N_2 system. The results demonstrated that cell density increased with saturation pressure because of increasing gas concentration. They investigated the effect of external pressure on the nucleation process. The results showed that the external pressure did not affect the cell number density (it was initially believed that the external pressure would decrease the cell number density because of a decreasing degree of supersaturation). The decrease in the gas solubility in PS as the saturated sample was heated above the T_g of the polymer could compensate for an increasing supersaturation degree, which could act as a driving force for the nucleation of cells.

Ramesh et al.[5] presented experimental and theoretical studies of the effect of various process conditions on cell growth in a PS–N_2 system. They reported that the cell growth rate increased with increase in the heating temperature because of the decreasing solution viscosity and increasing gas diffusivity. The cell size decreased with increase in the saturation pressure. As was reported by Kumar and Suh,[4] the number of nucleated cells increased exponentially with increase in the saturation pressure. It caused the growing cell to reach a smaller equilibrium cell size due to the limiting of the gas concentration in the polymer after the nucleation of the cells. They claimed that the deviation between theoretical and experimental results was caused by an interaction between the bubbles, which was not considered in their model.

Collias and Baird[6] investigated the deformation characteristics of PS by the presence of supersaturated nitrogen. They hypothesized that the release of nitrogen pressure after saturation created some tiny bubbles, but these vanished as nitrogen diffused out of the samples. The results demonstrated that the time scale of the change in the craze flow stress and corresponding percent elongation was equal to the diffusion time scale of nitrogen in PS, that is, 3 days. They concluded that the presence of nitrogen affected the deformation of PS, although not too significantly. The microcellular plastic, resulting in their experiment under applied process conditions, had a bubble size of 10 μm and a volume expansion of 25%.

In the previous studies on microcellular PS, the saturation process was usually conducted around room temperature, where the solubility of the gases is relatively high, but it needs a long time to reach saturation conditions. Variation in the saturation pressures will only affect the saturation concentration. Although increasing saturation temperature can reduce saturation time, the solubility of gases will generally drop at a high temperature. Based on the solubility data reported by Sato et al.,[7, 8] this phenomenon, however, is not fully valid for the PS–N_2 system. The solubility of N_2 decreases with increase in the temperature, but increases above about 350 K, showing so-called reverse solubility for various saturation pressures. Since the temperature change affected the gas concentration, it also affected cell nucleation and the cell growth rate because of the changing diffusion coefficient of the gas. Considering that the concentration of gas in the polymer plays a predominant role in the nucleation of cells, processing at various temperatures above room temperature might have a significant effect on the cell structure in the PS–N_2 system. In addition, increasing temperature will cause the viscosity of the polymer to significantly decrease, especially by the presence of gas swelling the polymer. Therefore, in this work, the effects of various saturation temperatures above room temperature were studied under a constant saturation pressure of 25 MPa. We propose a quick-heating method to investigate the variation in saturation pressure and heating time on the cell structure; the saturation temperature was kept constant at 393 K (above the T_g of PS). Quick-heating is the heating of a polymer without a time interval after decompression by the heat capacity of the saturation vessel. The degree of supersaturation of the saturated solution by quick-heating should be higher than that by late-heating, since the heating process by quick-heating started at the saturation concentration.[9,10] The results were compared with those of the usual late-heating method used by previous authors, that is, that which heats the saturated sample after an elapsed time since decompression. A long heating

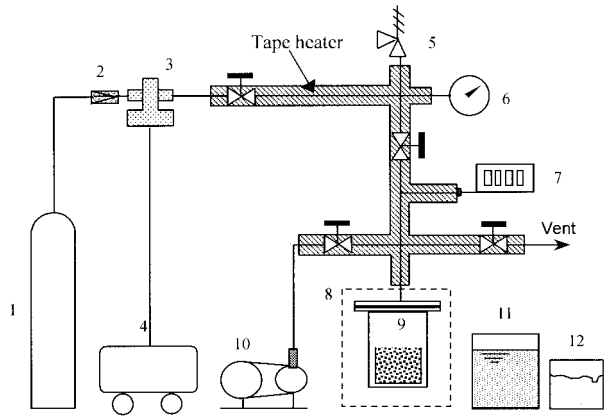

1. N_2 cylinder
2. Filter
3. Gas booster
4. Air compressor
5. Safety valve
6. Pressure gauge
7. Pressure indicator
8. Air bath
9. High-pressure vessel
10. Vacuum pump
11. Heating oil bath
12. Ice-water bath

Figure 1 Schematic diagram of the experimental apparatus for producing microcellular foam plastic.

time was studied to understand the microcellular structure change due to cell nucleation, cell growth, cell unification, and cell/foamed shrinkage.

EXPERIMENTAL

PS (Idemitsu Petrochemicals (Ichihara, Japan), HH30, M_w = 276,000) was used with nitrogen as a blowing agent (Iwatani Industrial Gases, Hiroshima, Japan, 99.9%). The gas was used as received without further treatment. The polymer was obtained as sheet samples with a thickness of about 1.3 mm; they were cut into 15 × 15-mm pieces. The sample pieces were annealed under 403 K in a vacuum oven for 12 h and cooled slowly to room temperature.

A schematic diagram of the experimental arrangement used in this work is sketched in Figure 1. First, the samples were placed in the saturation vessel immersed in an air bath. The vessel was evacuated and then charged with nitrogen gas up to a desired saturation pressure at a saturation temperature. When the period of saturation time was reached, the pressure was quickly released to atmospheric pressure. The present work examined two heating methods, that is, "late-heating" and "quick-heating." A sketch of the late-heating method and sample placement

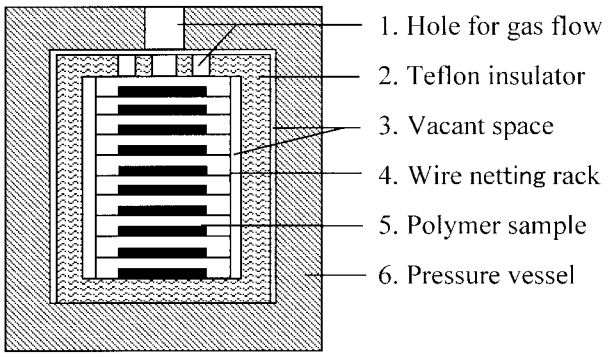

Figure 2 Setup of apparatus and sample placement inside the pressure vessel for "late-heating" method.

inside the saturation vessel is indicated in Figure 2. The samples were placed on a wire rack; they were thermally insulated from the wall of the vessel by a Teflon insulator to prevent convective heating after decompression. In the late-heating method, the samples were immediately taken out of the vessel (we needed at least 30 s to do it) after decompression. After a time interval (3 min since decompression), they were heated in a silicon oil bath at a foaming temperature for a certain heating time, then immersed in an ice-water bath.

The schematic of the quick-heating setup of the apparatus and polymer sample placement in the saturation vessel is presented in Figure 3. Instead of using the Teflon insulator, the samples were placed on brass trays. After decompression, the samples were kept in the vessel for a desired heating time to heat the samples by the heat capacity of the trays and vessel. After the heating process, cold water was delivered into the vessel to terminate the heating process. After the microcellular process, the samples were exposed to the atmosphere for over 1 week prior to the density

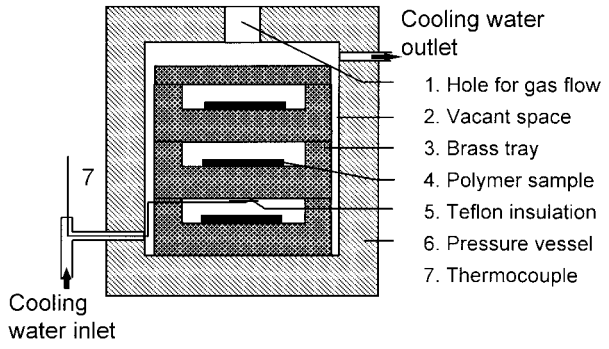

Figure 3 Setup of apparatus and sample placement inside the pressure vessel for "quick-heating" method.

measurement to ensure that the weight and volume of the sample had become constant. A part of the sample was then frozen and fractured in liquid nitrogen for microstructure analysis with SEM. The SEM image photographs were taken into a computer to obtain the cell size and cell distribution. The cell number density was evaluated according to Kumar and Suh.[4]

The bulk density of the samples was measured to determine the volume change of the samples before and after the microcellular process. The measurement was performed by the buoyancy method at 303 K. The volume expansion ratio, *VE*, is defined by the following equation:

$$VE = \frac{V_f - V_i}{V_i} \times 100\% \quad (1)$$

where V_i is the initial volume of the polymer sample, and V_f, the volume of the foamed sample. The data of the volume expansion ratio was compared with the ideal volume expansion to estimate the gas used to expand the sample. The ideal value was estimated from the volume of the amount of dissolved gas, which was taken from the gas solubility data.[7,8] The volume of gas was calculated at the heating temperature and at 0.1 MPa with the assumption that all dissolved gases were used for the expansion of the polymer. The ideal volume expansion, VE_{ideal}, was calculated as

$$VE_{\text{ideal}} = \frac{RT}{P}\frac{S}{M_w}\rho_{\text{pol}} \quad (2)$$

where R is the gas constant (cm^3 bar mol^{-1} K^{-1}); S, the solubility of gas in the polymer (g-gas/g-polymer); M_w, the molecular weight of the gas; and ρ_{pol}, the density of the neat polymer sample at room temperature (before foaming).

Figure 4 shows an example of a temperature profile during and after the decompression process of both heating methods. In decompression, the temperature inside the vessel decreases significantly because of the adiabatic expansion of the gas, then increases due to the heat conduction and radiation from the vessel. It is seen that the temperature change in quick-heating returns to almost the initial saturation temperature faster than in the late-heating method. The degree of supersaturation by quick-heating will be higher than by late-heating, since the heating process can be started while the gas concentration is still high. The difference in the two temperature profiles as well as the gas concentration in the heating process will cause different microcellular structures in the resulting samples.

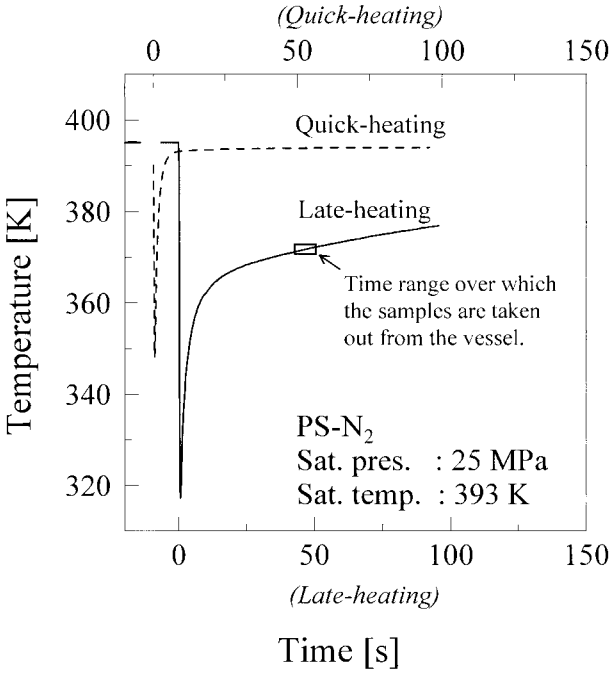

Figure 4 Profile of temperature change along and after decompression.

RESULTS AND DISCUSSION

Effect of Saturation Temperature

First, we investigated the effect of high saturation temperature on the microcellular cell structure with the conventional late-heating method. Figure 5 shows the results of experiments at a saturation pressure of 25 MPa, a heating temperature of 393 K, and a heating time in the oil bath for 30 s. The cell number density has a minimum and the mean cell diameter has a maximum around 350 K; the temperature of the minimum solubility of nitrogen in PS is as reported by Sato et al.[7, 8] The solubility of nitrogen in PS over a wide range of temperature and pressure was predicted with the Sanchez–Lacombe equation of state[11,12] based on the experimental results of Sato et al.[7, 8] and is shown in Figure 6. It is seen that above 350 K nitrogen solubility increases with increase in the temperature. The relationship of the solubility of nitrogen or the number of dissolved gases in PS to the cell structure exhibits good consistency up to about 393 K, but above this temperature, it shows

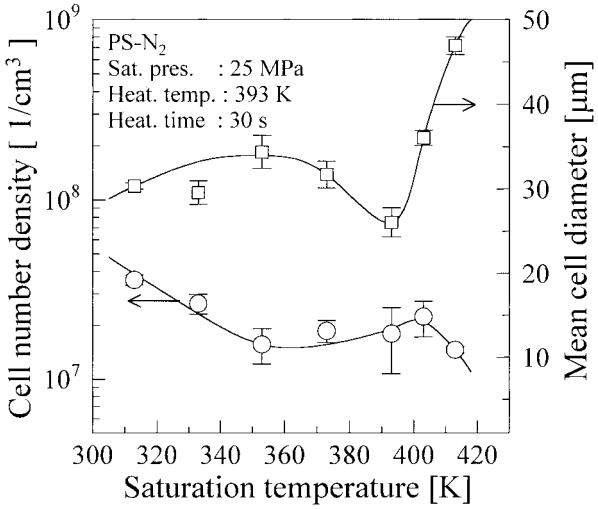

Figure 5 Effect of saturation temperature on cell structure (late-heating).

a discrepancy. Increasing the amount of gas increases the nucleation rate of cells; as a result, the cell number density increases and the cell diameter decreases because of the limiting amount of gas for growing. Above 393 K, besides increasing the dissolved gas in the polymer, the solution and vessel temperature are too high. Since the T_g of the polymer decreases with increase in the gas concentration in the polymer, when decompression is performed from a high saturation temperature, cell nucleation, cell unification, and cell growth occur before removal from the vessel. The heating process in silicon oil just increases the length of heating time and causes an increase in the unification and growth of cells. As a result, the cell number density decreases and the mean cell diameter increases.

The above results agree with the classical nucleation theory according to which the cell nucleation rate is linearly related to the gas concentration in the polymer and is expressed as

$$N_{\text{hom}} = Z\beta^* C_0 \exp(-\Delta G^*_{\text{hom}}/kT) \qquad (3)$$

where N_{hom} is the homogeneous nucleation rate; Z, the Zeldovich factor; β^* , the joint rate of molecules; C_0, the concentration of gas molecules in the polymer; ΔG^*_{hom}, the Gibbs free energy changing for homogeneous nucleation; k, the Boltzmann's constant; and T, the absolute temperature.[2,3,13] Discussion of this calculation method can be found in the Appendix. The dissolved gas in the polymer swells the polymer matrices so that the polymer chains can freely move and interact with each other. The viscosity and surface tension of the polymer–gas solution reduces to below the pure polymer at the same temperature. Consequently, increasing gas concentration leads to decreasing the critical radius and the Gibbs energy of nucleation. An increasing cell nucleation rate results in an increase in cell number density and a decrease in the mean cell diameter. A comparison of the experimental results with the theoretical calculation results is shown in Figure 7. Both results show agreement except above 393 K, which indicates that classical nucleation theory is applicable only under conditions where the unification of the cell has not occurred. Below 350 K, the minimum temperature of the nitrogen solubility in PS and the dependence of the cell number density on the gas concentration can be seen more clearly than above 350 K. This occurs because the amount of gas that escapes before heating is greater for samples processed above 350 K. Therefore, the amount of dissolved gas used for nucleation and growth might not be as much as for samples processed below 350 K. However, we can show a strong relationship between the gas solubility of the PS–N_2 system and the cell structure. It is possible to process microcellular plastic from a PS–N_2 system at higher temperature without the confusion of the decreasing solubility of gas. By carefully controlling the heating process,

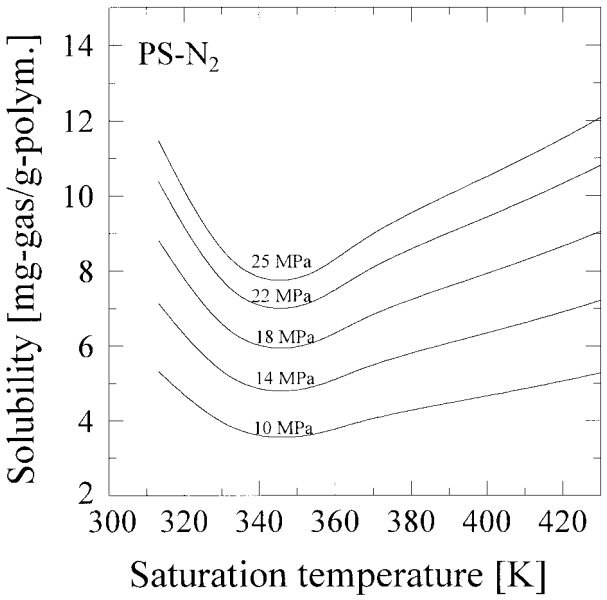

Figure 6 Solubility of nitrogen in PS (predicted by Sanchez–Lacombe EOS[11,12] with experimental data from Sato et al.[7,8]).

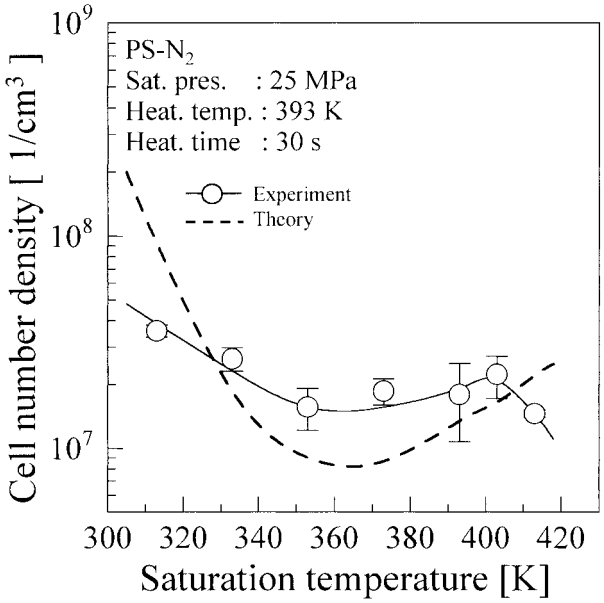

Figure 7 Effect of saturation temperature on cell structure; a comparison of theory and experimental results (late-heating).

microcellular plastics with a high cell number density and a small diameter can be produced.

The volume expansion ratio as a function of saturation temperature is shown in Figure 8. The broken line in this figure expresses an ideal value of the volume expansion ratio assuming that all the dissolved gas is used to expand the polymer as previously explained. The measured volume expansion reveals the same tendency as that of the gas solubility. This is reasonable if we consider that a part of the dissolved gas is used to expand the polymer and the rest of the gas diffuses out of the polymer. However, at the highest temperature in the experiment, the sample expanded about seven times as much as did the initial volume. This might be caused by an increase in the cell growth rate due to the sudden reduction of polymer viscosity above the glass transition temperature. Visually, the microcellular structure change by the saturation temperature change is shown in Figure 9. The effects of saturation temperature related to gas solubility are shown in this figure. Because the gas solubility was higher at 313 K (a) than around the minimum solubility at 353 K (b), the cell size was smaller and the cell number density was higher. Increasing the gas solubility above 350 K caused an increase in cell number density and a slight decrease in cell diameter, which is shown in Figure 9(c). When the saturation process was performed below 413 K, cell growth and the unification of cells caused the cell diameter to increase and the cell number density to decrease, as shown in Figure 9(d).

From these results, we conclude that microcellular PS, having many small cells and low density, can be produced at high temperature with nitrogen as a blowing agent. This information is valuable for industrial production of microcellular plastics, because continuous processes are operated at high temperatures around the melting temperature of polymers.

Effect of Saturation Pressure

The effect of the saturation pressure on the microcellular structure was investigated at a high saturation temperature of 393 K with both the late- and quick-heating methods. Heating temperature and heating time were kept constant at 393 K and 30 s. For quick heating, the saturation temperature is the same as the heating temperature; therefore, it is performed above the T_g of PS. Figure 10 shows the solubility of nitrogen in PS at 393 K, which was predicted by the Sanchez–Lacombe equation of state[11,12] with experimental data from Sato et al.[7,8] The solubility increases linearly with pressure up to about 25 MPa.

Variation of the microcellular structure with saturation pressure is presented in Figure 11 with SEM images in Figure 12. The cell number density increases and the mean cell diameter de-

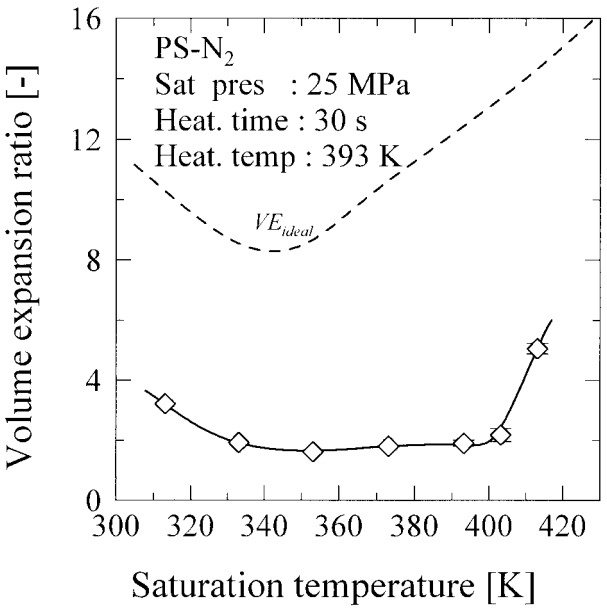

Figure 8 Effect of saturation temperature on volume expansion ratio (late-heating).

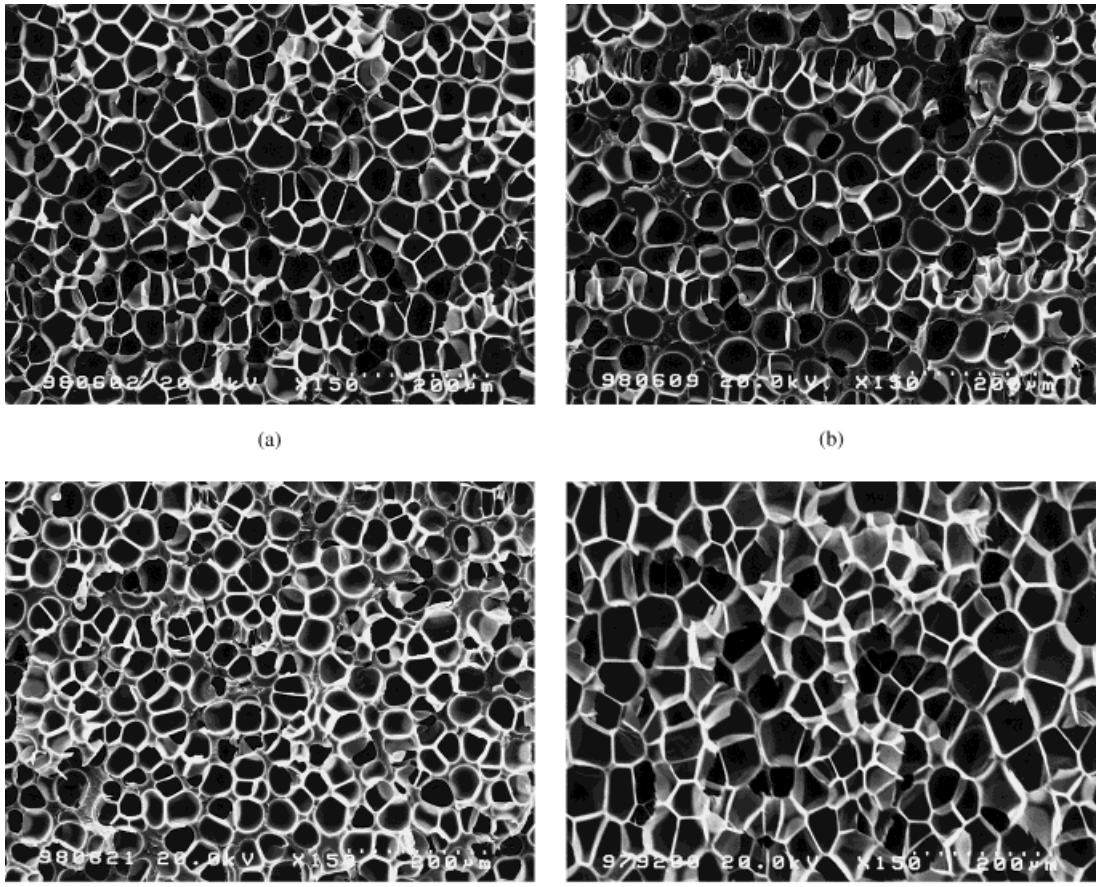

Figure 9 SEM photographs show the effect of saturation temperature on cell structure.

creases with increase in the saturation pressure, namely, with increase in the gas solubility in the polymer. The reason for this solubility effect is the same as that previously mentioned. These results agree with those reported by Kumar and Suh.[4] The cell number density of the sample processed under the quick-heating method is slightly higher, while the cell diameter is significantly larger than in late-heating. This means that the nucleation rate of both methods is relatively similar. At the applied saturation temperature (393 K), the nucleation of the cells is almost completed at decompression and/or at initial time before removal from the vessel. This is reasonable since 393 K is above the T_g of PS. The difference in the degree of supersaturation, contributed by faster heating in the quick-heating method, led to a slightly higher cell number density. The larger mean cell diameter in quick-heating might be due to the higher gas concentration available in the polymer and the higher cell growth rate because of the higher gas diffusion coefficient. The photographs of the sample processed by both heating methods show that, for the same applied process conditions, the mean cell diameter of the sample processed under quick-heating is larger than in late-heating. The quick-heating process only enhanced the growth rate of the cells, which is clearly shown in Figure 12(a–c). By increasing the saturation pressures, the mean cell diameter of quick-heating was larger, while the cell number density was almost the same.

The difference in the cell growth rate in the two heating processes was more clearly observed in the volume expansion data shown in Figure 13. The microcellular samples produced with the quick-heating method expanded about three times as much as those processed with the late-heating method. A comparison of the ideal volume expansion shown by the broken line with the ex-

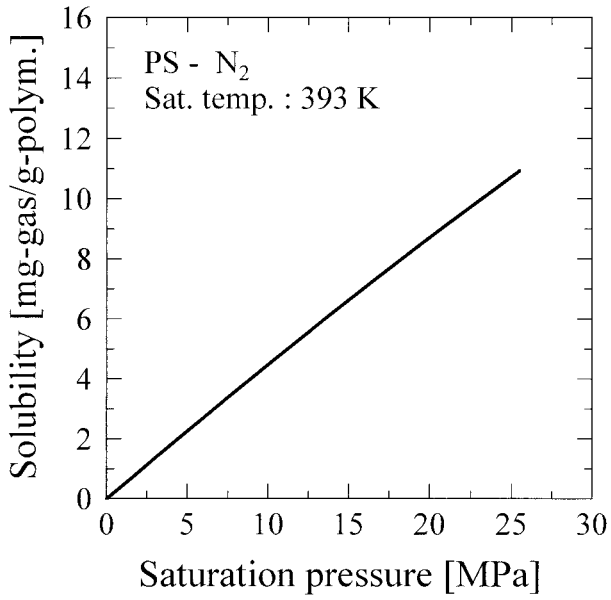

Figure 10 Solubility of nitrogen in PS at 393 K (predicted by Sanchez–Lacombe EOS with experimental data from Sato et al.[7,8]).

perimental values indicates that only about 10% of the dissolved gas was used to expand the polymer samples in the late-heating method. The remaining about 90% of the dissolved gas had diffused out of the sample. However, in the case of the quick-heating method, the amount of gas used to expand the polymer is more than 30% of the total dissolved gas. A simple calculation may tell us that about 20% of the dissolved gas diffused out of the polymer during the 3 min between the end of the decompression process and the beginning of the heating process in the oil bath. This result proves that there is a higher gas concentration in the quick-heating process than in the late-heating process.

Effect of Heating Time

The dynamic change in cell structure as a function of the heating time in the two heating methods is presented in Figure 14. There are three different stages: the first stage up to 30 s, the second stage from 30 to about 300 s, and the final stage over 300 s. In the first stage, the cell number density appears almost constant, and the mean cell diameter increases due to cell growth, that is, the diffusion of gas molecules from the bulk polymer into the nuclei. Almost constant values of the cell number density may denote that a large part of the cells are nucleated during the early stage of heating. The nucleation rate of the cells becomes quite low, because of the decreasing

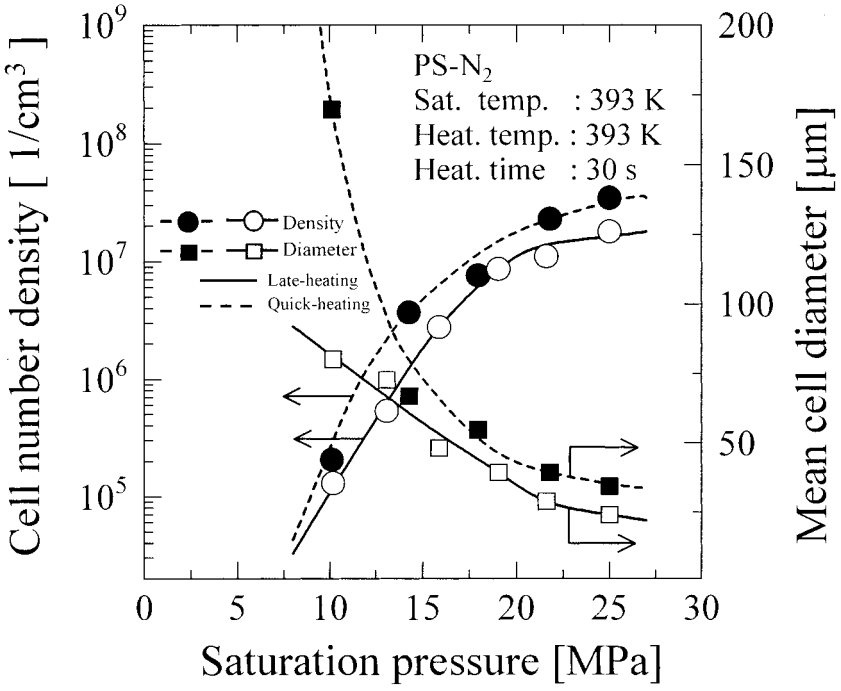

Figure 11 Effect of saturation pressure on cell structure (a comparison of late- and quick-heating).

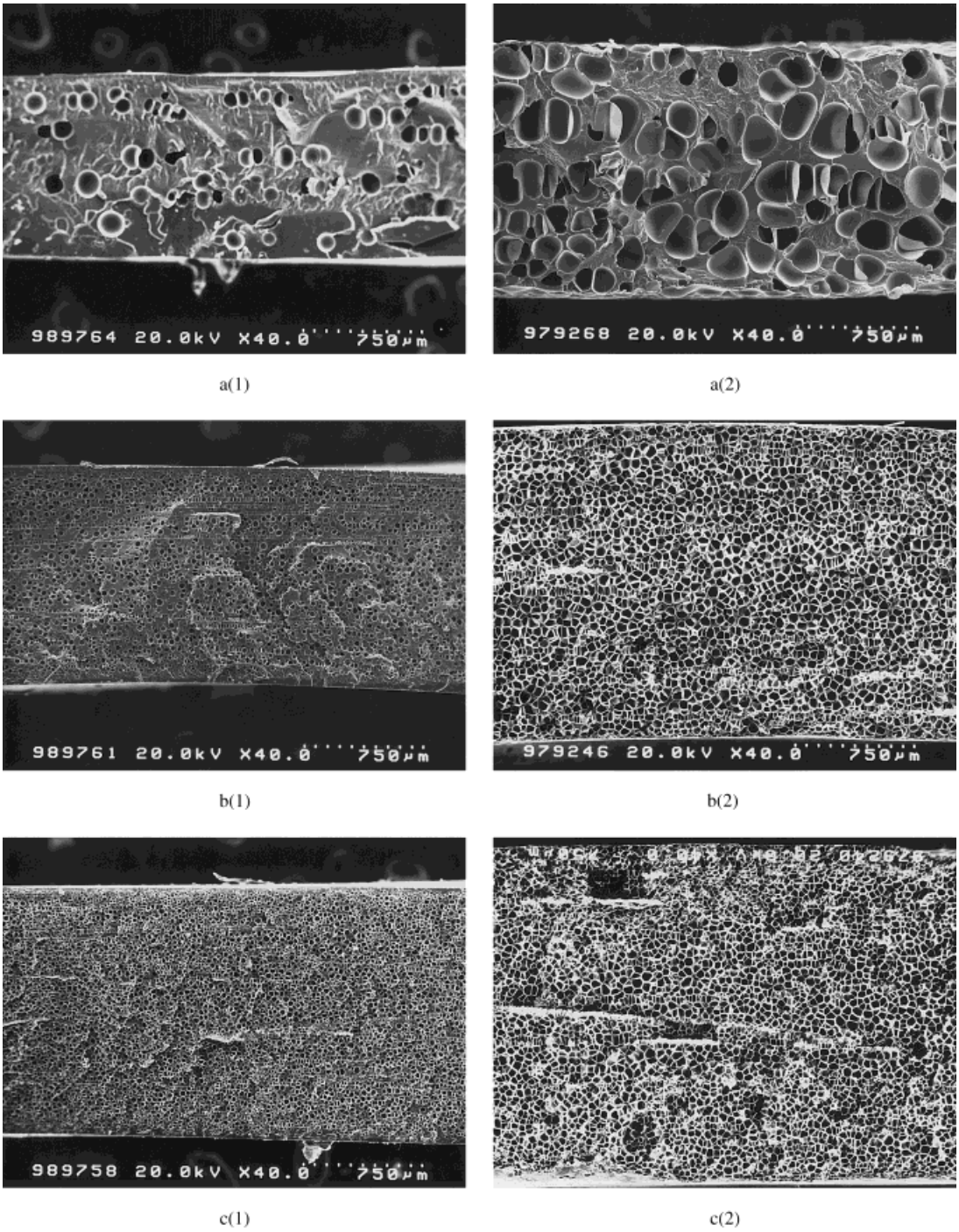

Figure 12 SEM photographs show the effect of saturation pressure under late- and quick-heating at 393 K and 30 s.

gas concentration in the polymer. The cell number density then decreases in the second stage due to the unification of two or more cells. Therefore, the mean cell diameter increases because of the cell growth and the unification. Ramesh et al.[6] reported that the mean cell diameter reached an equilibrium value after a heating time of 120 s (heating/foaming temperature was 388 K) and was not changed up to 300 s, because of the depleted gas concentration in the polymer. How-

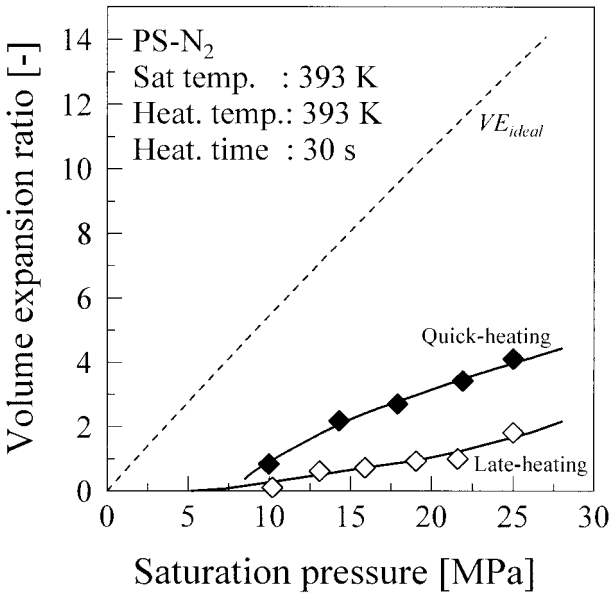

Figure 13 Effect of saturation pressure on the volume expansion ratio (a comparison of late- and quick-heating).

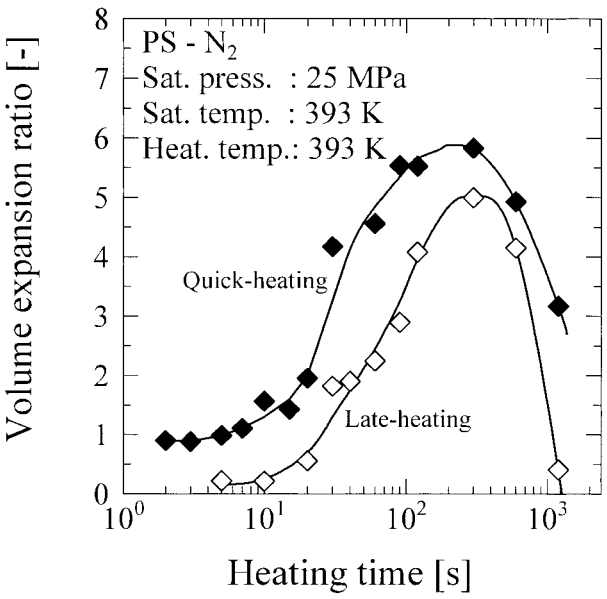

Figure 15 Effect of heating time on the volume expansion ratio (a comparison of late- and quick-heating).

ever, we obtained another result after the second stage. In the final stage, the cells number density decreased, and the mean cell diameter increased slowly with time. The decrease in the cell number density is caused by the unification of cells, while increase in the mean cell diameter may indicate the growth of cells. It is quite reasonable to consider that the gas molecules in the cells tend to diffuse out of the polymer after the depletion of the gas pressure in the polymer, because of the higher pressure in the cells and a higher gas concentration in the sample than in the atmosphere. The shrinkage of cells will be proved by the change in the ample volume expansion ratio as shown in Figure 15. The volume expansion ratio increased during the first and second stages. However, in the final stage, foamed polymer volumes were drastically reduced.

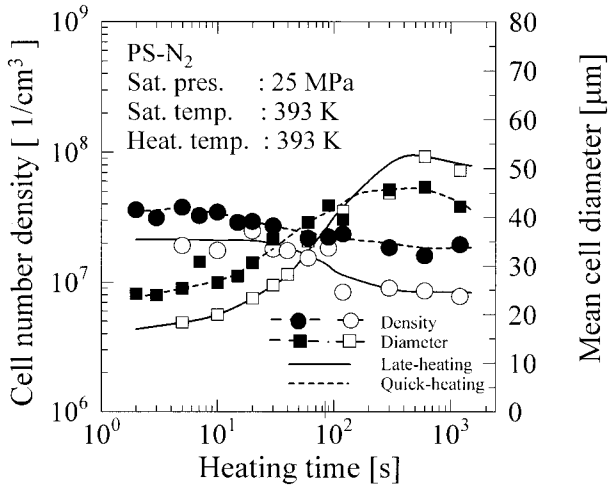

Figure 14 Dynamic change of cell structure by heating time (a comparison of late- and quick-heating).

In the quick-heating method, the change in cell number density and mean cell diameter with heating time was relatively small. Large cell number densities may be influenced by the high nucleation rate in the initial time of the first stage, while the larger mean cell diameter is caused by the higher growth rate. As previously mentioned, quick-heating at high gas concentration enhanced the nucleation and growth rate of the cells. In the second stage, the experimentally obtained mean cell diameters were still larger than those by the late-heating; however, over 150 s, the mean cell diameter was smaller, which means that the cell growth rate had slowed. These results, as well as the volume expansion ratios shown in Figure 15, indicate an almost constant volume expansion ratio over 150 s, which reaches a maximum around 300 s. Since the total number of gas molecules were primarily used for the nucleation of cells, the mean cell diameter in the final stage of the quick-heating process was smaller than that of the late-heating process, but the cell number density was higher.

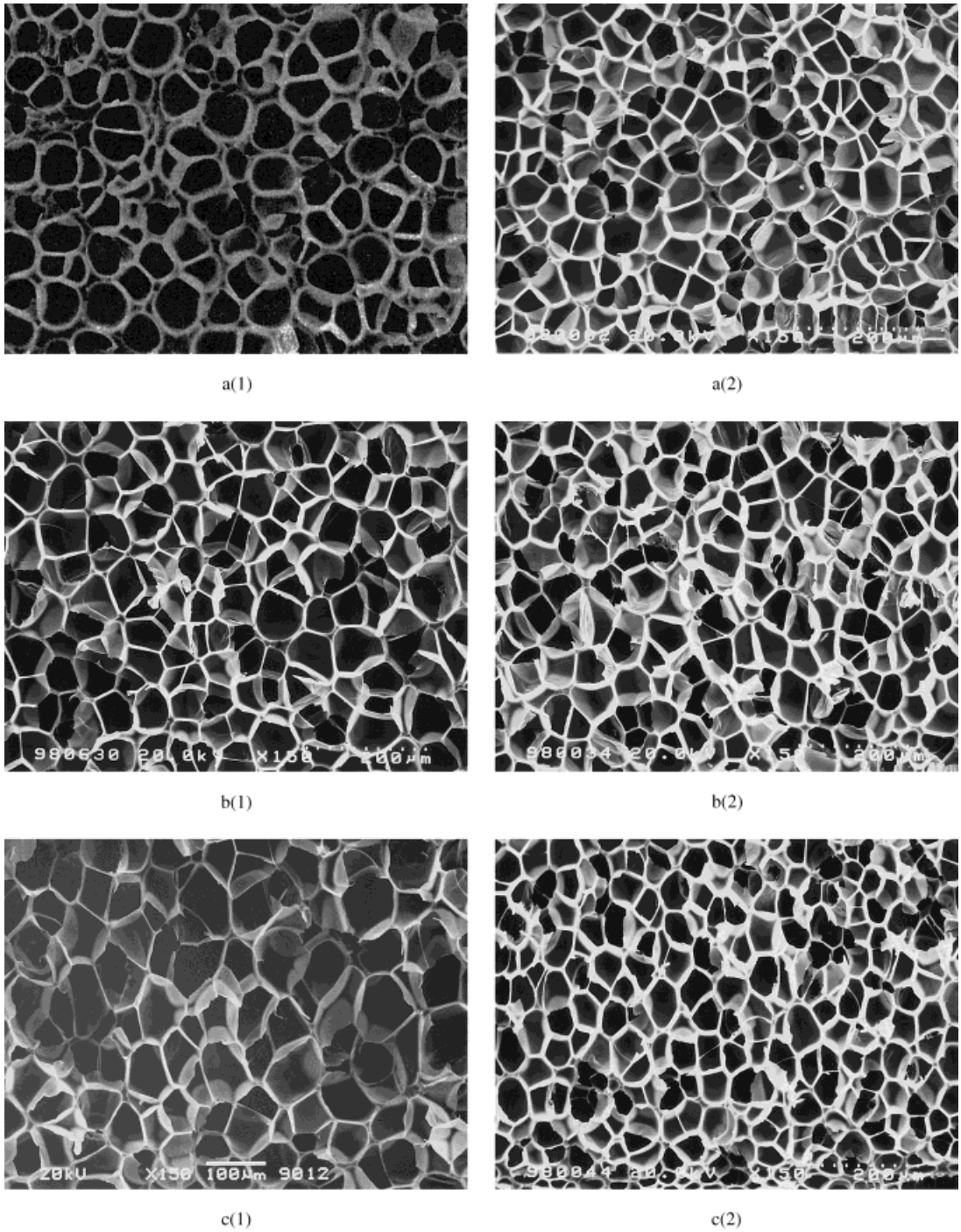

Figure 16 SEM photographs show the effect of heating time under late- and quick-heating.

The typical cell structure change with heating time under both heating methods is visually shown in Figure 16. It is clearly shown that, for heating time up to 30 s under the quick-heating process, the mean cell diameter is larger and the cell number density is higher than in late-heating [Fig. 16 (a)]. At 600 s (over 300 s, i.e., the maximum mean cell diameter), a reverse condition appears: The mean cell diameter of the quick-heating process is smaller, but the cell number

density is higher [Fig. 16 (b)]. When the heating process was continued up to 1200 s, the quick-heating process reached a final cell size smaller than in the late-heating process and higher mean cell number density [Fig. 16 (c)]. These facts demonstrate that the quick-heating process could increase the degree of supersaturation of the polymer solution.

CONCLUSIONS

The effects of saturation pressure, saturation temperature, heating time, and heating method on the cell structure were studied for PS microcellular plastic production. The solubility of gas, which is related to saturation pressure and temperature, had a significant effect on the structure of microcellular plastics. Increasing gas solubility increased the cell number density and reduced the cell size. The heating time could be used as a controlling variable to obtain a desired cell structure and volume expansion ratio. Application of the quick-heating process enhanced the degree of supersaturation of the polymer–gas solution, resulting in a small equilibrium cell size, high cell number density, and volume expansion ratio.

The authors wish to thank the Hiroshima Industrial Technology Organization and Japan Science and Technology Corp. for providing financial support.

APPENDIX

The interfacial tension of the polymer–gas solution, γ_{mix}, was calculated by an equation derived by Goel and Beckman.[13] By considering that the surface tension of high-pressure gases is much smaller than that of the polymer, that the saturation process is performed above the glass transition temperature of the PS, and that nitrogen gas is dissolved in the PS, the surface tension of the mixture was treated as

$$\gamma_{mix} = \gamma_p \left[\frac{\rho_{mix}}{\rho_p} \right]^4 (1 - w_g)^4 \quad (A.1)$$

where γ_p and ρ_p are the surface tension and density of the pure polymer, respectively; ρ_{mix}, the density of the gas–polymer mixture; and w_g, the weight fraction of the gas in the polymer.

The density of PS was estimated from the equation by Ruud[14]:

Below the T_g:

$$\rho_T = \rho_{298} - 2.65 \times 10^{-4}(T - 298.15) \quad (A.2)$$

Above the T_g:

$$\rho_T = \rho_{298} - 6.054 \times 10^{-4}(T - 298.15) \quad (A.3)$$

where ρ is in the unit of g/cm^3 and T in K. The surface tension of pure PS at various temperatures was calculated according to Van Krevelen[15]:

$$\gamma_T = \gamma_{298}(\rho_T/\rho_{298})^4 \quad (A.4)$$

The solubility data of nitrogen in PS by Sato et al.[7,8] was used to obtain w_{gas}. The change in polymer density due to the dissolved gas was calculated by the application of a simple mixing rule as

$$\rho_{mix} = \frac{\rho_p \rho_g}{w_p \rho_g + w_g \rho_p} \quad (A.5)$$

Z in eq. (3) was as calculated according to Russel.[16] β^* was calculated based on Reis[17] as

$$\beta^* = \frac{3D}{2\bar{l}} C_0 \quad (A.6)$$

where D is the diffusion coefficient of gas in the polymer; $\bar{l}$, the distance between the adjacent molecules; and C_0, the saturated concentration of gas in the polymer.

REFERENCES

1. Baldwin, D. F; Tate, D. E.; Park, C. B.; Cha, S. W.; Suh, N. P. J Jpn Soc Polym Proc 1994, 6, 187, 245.
2. Martini, J.; Waldman, F.; A. Suh, N. P. In Proceedings of the SPE ANTEC '82, May 1982; p 674.
3. Colton, J. S.; Suh, N. P. Polym Eng Sci 1987, 27, 493.
4. Kumar, V.; Suh, N. P. Polym Eng Sci 1990, 30, 1323.
5. Ramesh, N. S.; Rasmussen, D. H.; Campbell, G. A. Polym Eng Sci 1991, 31, 1657.
6. Collias, D. I.; Baird, D. G. Polym Eng Sci 1996, 35, 1167.

7. Sato, Y.; Yurugi, M.; Fujiwara, K.; Takishima, S.; Masuoka, H. Fluid Phase Equilib 1996, 125, 129.
8. Sato, Y.; Fujiwara, K.; Takikawa, T.; Sumarno; Takishima, S; Masuoka, H. Fluid Phase Equilib 1999, 162, 261.
9. Sumarno, Hayashi, K.; Sato, Y.; Takishima, S.; Masuoka, H. In Proceedings of the 5th Meeting on Supercritical Fluids, Tome 1: Materials, Nice, France, 1998; p 33.
10. Sumarno; Hayashi, K.; Sato, Y.; Takishima, S.; Masuoka, H. In Proceedings of the PPS-14 Annual Meeting, Yokohama, Japan, 1998; p 617.
11. Sanchez, I. C.; Lacombe, R. H. J Phys. Chem 1976, 80, 2352.
12. Sanchez, I. C.; Lacombe, R. H. Macromolecules 1978, 11, 1145.
13. Goel, S. K.; Beckman, E. C. Polym Eng Sci 1994, 34, 1137.
14. Ruud, F. J. In Polymer Handbook; Bandrup, J.; Immergut, E. H.; Wiley: New York, 1967.
15. Van Krevelen, D. W. Properties of Polymers; Elsevier: New York, 1976.
16. Russel, K. C. Adv Colloids Interf Sci 1980, 13, 205.
17. Reis, H. J. Chem Phys 1950, 18, 996.